FISEVIER

Contents lists available at ScienceDirect

### **Optics Communications**

journal homepage: www.elsevier.com/locate/optcom



# Robust design of broadband EUV multilayer using multi-objective evolutionary algorithm



Shang-qi Kuang a,\*, Xue-peng Gong b, Hai-gui Yang c

- <sup>a</sup> School of Science, Changchun University of Science and Technology, Changchun 130022, China
- b State Key Laboratory of Applied Optics, Changchun Institute of Optics, Fine Mechanics and Physics, Chinese Academy of Sciences, Changchun 130033, China
- <sup>c</sup> Key Laboratory of Optical System Advanced Manufacturing Technology, Changchun Institute of Optics, Fine Mechanics and Physics, Chinese Academy of Sciences, Changchun 130033. China

ARTICLE INFO

Keywords: Multilayers Multilayer design X-ray Soft X-rays Extreme ultraviolet Thin films

#### ABSTRACT

Considering the random fluctuations of the layer thickness, a method of robust design of broadband EUV multilayers based on multi-objective evolutionary algorithm is presented. Owing to the optimization of multi-objective evolutionary algorithm, the optical performance and robust quality of broadband Mo/Si multilayer can be optimized simultaneously, and then a set of robust designs of aperiodic EUV multilayers, which are insensitive to the thickness errors can be obtained in one single simulation run. The robust designs of broadband Mo/Si multilayers could be used to reduce the production risks of EUV mirrors, and this research demonstrates a great potential of application of multi-objective evolutionary algorithm on the design of optical thin film.

© 2017 Elsevier B.V. All rights reserved.

### 1. Introduction

In the last three decades, the multilayer mirrors have been used in the development of next generation of lithography system for the semiconductor industry [1-3], but due to the narrow spectral and angular bandwidth of standard periodic multilayer, the range of their applications is limited. In many applications such as EUV metrology, X-ray astronomy and X-ray ultrashort pulses [4–7], it is desirable that either the spectral or angular bandwidth is essentially increased [8–10]. The way generally used to increase the reflectivity bandwidth of periodic multilayer is the variations of layer thicknesses in the multilayer, and such coating is defined as aperiodic multilayer or supermirror. The theoretical approaches for the design of broadband multilayer are based either on full numerical calculations [11-17] or numerical calculation with an appropriate initial structure [18-22]; and suitable algorithms such as evolutionary strategy [11-15], stimulated annealing algorithm [16,17], Levenberg-Marquardt [18-22], and particle swarm optimization [23] have been used. Among these optimization algorithms, the algorithms of Levenberg-Marquardt and evolutionary strategy are widely used. It can be expected that better multilayer designs should be obtained when the thickness of each layer is considered as an independent variable. Under this consideration, the multilayer design spans a whole solution space in principle, and the better reflectivity performance can be found. However, due to the large amount of independent parameters, the Levenberg–Marquardt algorithm usually tends to get trapped in the local minima, and the achievement of globally optimum usually depends on the choice of initial multilayer structure [18–22]. By contrast, the evolutionary strategy such as genetic algorithm is a more suitable approach to the optimization of broadband multilayer when all the layer thicknesses are allowed to modulate, because this algorithm is a global optimization method, and a near-optimum solution can be found in an acceptable calculation time [11–15].

We realize that it is not very difficult to obtain a desirable thickness distribution with the algorithms above mentioned, and there are a number of different thickness distributions that can provide the similar reflectivity profile within a prescribed accuracy, but these multilayer designs give different performances when random thickness errors are considered. It is found that random thickness errors which originate from imprecision deposited control could lead to a deformation of the reflectivity curve [10,18]. Many researches have been carried out to consider the influences of random thickness errors on the optical performance in the optimization procedures, and a robust multilayer design whose optical performance is insensitive to the thickness errors can be obtained [24–26]. In the optimization procedure of traditional design, only the optical performance is the optimized objective, and optical performance of obtained multilayer design is usually sensitive to the random thickness errors. While in the optimization procedure of robust

E-mail address: physicskuang@sina.com (S.-q. Kuang).

<sup>\*</sup> Corresponding author.

design, the robust quality is set as the optimized objective, but optical performance of obtained multilayer design usually cannot be acceptable. Therefore, we realize that the optical and robust performances of multilayer should be equally important in the fabrication, and both objectives should be considered simultaneously in the procedure of multilayer design. Though it is simple to convert these two optimized objectives into a single goal, which just optimizes the summation of two merit functions, but it often fails to reflect the complex relationship between objectives and one must give a good consideration of weight between two objectives. During recent years, a multi-objective evolutionary algorithm which is defined as non-dominated sorting genetic algorithm II (NSGA-II) has been developed, and much better performance of NSGA-II for multi-objective optimization problem is observed [27]. This algorithm can simultaneously optimize two objectives, and due to the advantage of evolutionary algorithm, it is immune to local topology in the solution space. Furthermore, during the optimization of NSGA-II, these two objectives do not influence each other, and this algorithm has the ability to find a good convergence near the true Pareto-optimal front which is a set of solutions of the multi-objective problem.

In this paper, a procedure for the robust design of broadband EUV multilayer is presented, and the reflectivity and robust performances of the aperiodic Mo/Si multilayer are set as two objectives of NSGA-II. This research should open the application of multi-objective evolutionary algorithm on the design of optical multilayer, and this set of mathematical procedures also has a great potential to give other multilayer designs which combine other optical performances. It is worthwhile to point out that the ultra-smooth substrate of EUV multilayer is high cost, thus this robust multilayer design of broadband Mo/Si multilayer could reduce the production risks of EUV mirrors.

## 2. Design of Mo/Si multilayer based on multi-objective evolutionary algorithm

At first, we present a brief description of electromagnetic wave propagation in a non-periodic multilayer system, and demonstrate the theoretical calculation of reflection. The wave propagation in a homogeneous layer j which is contained in the multilayer system can be characterized by transfer matrix  $\mathbf{M}_j$ , and this matrix which connects the electric field between the neighboring layers j and j+1 can be written by

$$\mathbf{M}_{j} = \mathbf{T}_{j} \cdot \mathbf{R}_{j,j+1} = \begin{bmatrix} e^{-ik_{j}d_{j}} & 0 \\ 0 & e^{ik_{j}d_{j}} \end{bmatrix} \cdot \begin{bmatrix} t_{j,j+1} & r_{j,j+1} \\ r_{j,j+1} & t_{j,j+1} \end{bmatrix}, \tag{1}$$

where  $\mathbf{T}_j$  and  $\mathbf{R}_{j,j+1}$  are the translation and refraction matrices, respectively. Here,  $d_j$  is the layer thickness, and the coefficients  $r_{j,j+1}$  and  $t_{j,j+1}$  should be given as

$$\begin{split} r_{j,j+1} &= \frac{k_{j+1} - k_j}{2k_{j+1}}; \\ t_{j,j+1} &= \frac{k_{j+1} + k_j}{2k_{j+1}}, \end{split} \tag{2}$$

where  $k_j$  represents the z-component of wave-vector for layer j. In the general case, the value of  $k_j$  depends on the polarization of the incident radiation, and it can be given as

$$k_{j} = \begin{cases} \frac{2\pi}{\lambda} n_{j} \cos \theta_{j} & \text{s polarization,} \\ \frac{2\pi}{\lambda} \frac{n_{j}}{\cos \theta_{j}} & \text{p polarization;} \end{cases}$$
(3)

where  $n_j = 1 - \alpha_j - i\beta_j$  is the complex refractive index of the layer j,  $\theta_j$  is the incident angle of the layer j,  $\lambda$  is the incident beam wavelength, and here the optical constants are taken from CXRO database [28].

Considering the loss in reflectance due to interfacial roughness, the coefficient  $r_{i,j+1}$  in Eq. (1) should be modified by

$$\widetilde{r}_{j,j+1} = r_{j,j+1} \exp \left[ -2n_j \cos \theta_j n_{j+1} \cos \theta_{j+1} \left( \frac{2\pi \sigma_{j,j+1}}{\lambda} \right)^2 \right], \tag{4}$$

where  $\sigma_{j,j+1}$  is the interfacial roughness between the layers j and j+1. When the electromagnetic wave propagates through a multilayer system with N layers, the propagation should be represented by the characteristic matrix [29]

$$\mathbf{M} = \begin{bmatrix} M_{11} & M_{12} \\ M_{21} & M_{22} \end{bmatrix} = \mathbf{R}_{\text{sub}} \mathbf{M}_1 \cdots \mathbf{M}_j \cdots \mathbf{M}_N, \tag{5}$$

where  $\mathbf{R}_{\mathrm{sub}}$  is the refraction matrix between the substrate and first layer. For the EUV radiation, the Fresnel reflection coefficient of the electric field at the surface of the multilayer system can be given by

$$r_N = \frac{M_{12}}{M_{22}},\tag{6}$$

and then the reflectivity can be calculated by

$$R = |r_N|^2. (7)$$

Secondly, we demonstrate the mathematical procedure of robust multilayer design, which is based on NSGA-II. Here two merit functions of multilayer design can be defined by

$$f_1 = \int_{\varphi_{\min}}^{\varphi_{\max}} \left[ R(\varphi) - R_0 \right]^2 d\varphi;$$

$$f_2 = f_1 + \frac{1}{2} \sum_{i=1}^m \frac{\partial^2 f_1}{\partial d_i^2} \delta_i^2,$$
(8)

where R and  $R_0$  are the theoretical and target reflectivities of the design multilayer respectively, and then the first merit function  $f_1$  characterizes the root-mean-square deviation of the calculated reflectivity profile from the desired one. Here  $d_i$  and  $\delta_i$  are the thickness and thickness error's standard deviation of the ith layer respectively, thus the second merit function  $f_2$  is the robust design merit function of multilayer [25]. In Eq.(8), we consider m layers included in the multilayer system have thickness errors which originate from imprecision deposited control of quartz crystal monitoring or time monitoring. Therefore, these thickness errors are independent and can be simulated as random ones distributed in accordance with normal distribution law with zero mathematical expectation and standard deviations. Hence, the reflectivity performance of multilayer design is optimized by minimization of the first merit function  $f_1$ , and the multilayer design's sensitivity of reflectivity performance to layer thickness errors can be optimized by minimization of the second merit function  $f_2$ . In order to simultaneously optimize these two merit functions, both of them are set as the optimized objectives of NSGA-II, and each individual's gene is characterized by a set of parameters which are the layer thicknesses required optimizations. We use a population size of 100 and run the program until 3000 generations. Other parameters of the program are that the crossover probability  $P_c$ is 0.9, mutation probability  $P_{\rm m}$  is 0.1, and distribution indexes for the crossover and mutation operators are  $\eta_c = 2$  and  $\eta_m = 2$ , respectively. In the following, we demonstrate the conceptual steps of NSGA-II which can be applied to robust design of aperiodic Mo/Si multilayer, and much more details can be found in [27] and the references therein.

Step 1. Initialization of the internal multi-objective evolutionary algorithm settings. In this step, all the parameters above mentioned are assigned with values.

Step 2. Creation of a random parent population. Each solution in the population is represented by the multilayer's parameters of layer thicknesses which require the optimizations.

Step 3. Evaluation of the parent population, by calculating these two fitness functions in Eq.(8).

Step 4. Each parent solution is assigned a rank equal to its nondomination level, and the nondominated solutions are further sorted by using the crowding comparison procedure.

If both fitness values of solution p are less than that of solution q respectively, it is defined that solution q is dominated by solution p, which means solution p is superior to solution q; otherwise the relation between these two solutions is nondomination. In this step, each solution is compared with every other solution in the population

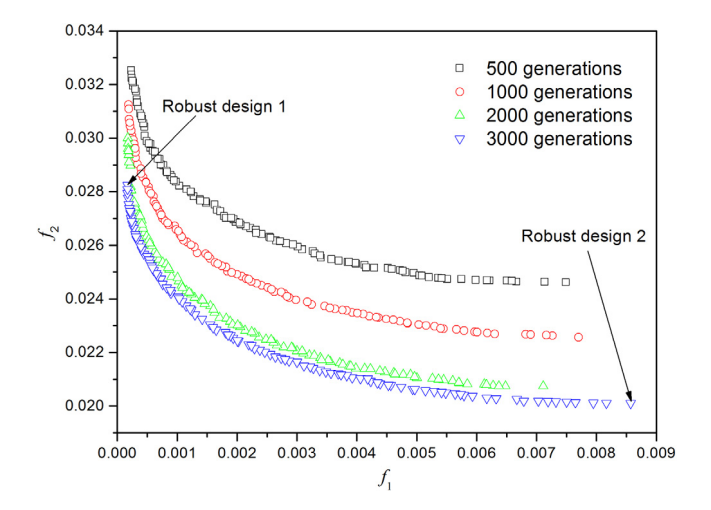


**Fig. 1.** Obtained nondominated solutions according to different generations of NSGA-II, where reflectivity and robust performances of multilayer design are set as two optimized objectives. The designed target of reflectivity performance of Mo/Si multilayer is the constant reflectivity  $R_0 = 52\%$  in the range of angle of incidence  $[0^\circ, 16^\circ]$  at a wavelength of 13.5 nm, and here s polarization of light is considered. These two boundary solutions in the nondominated front are defined as "Robust design 1" and "Robust design 2", respectively. Here the random thickness error of Mo or Si layer has the normal distributions and standard deviations of 0.1 nm.

to find if it is dominated, and this process is continued until all the solutions have finished the comparisons. After this process, one can identify the first set of nondominated solutions, which are defined in the first nondominated level or the first nondominated front. In order to find the individuals in the next nondominated front, the solutions of the first front are discounted temporarily and the above procedure is repeated. With this approach, a population can be sorted into different nondomination levels.

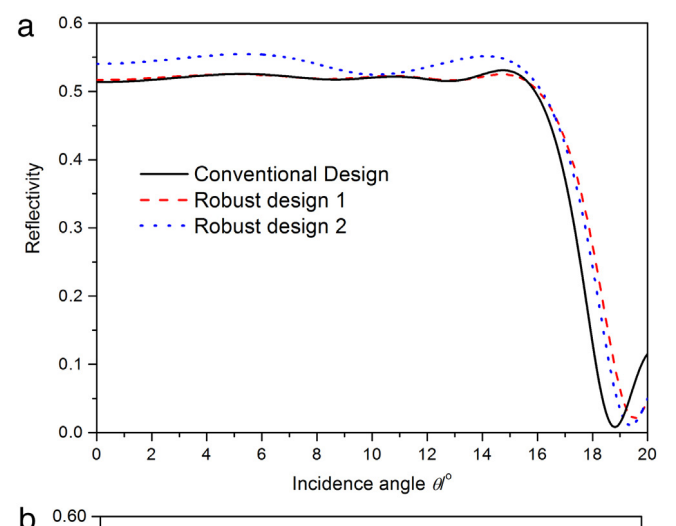
According to the solutions in the same nondominated level, we sort them by comparing their crowding distances. At first, these solutions are sorted according to each objective function value in ascending order of magnitude. Secondly, for each objective function, the boundary solutions are assigned an infinite distance value; other intermediate solutions are assigned a distance value equal to the absolute normalized difference in the function values of two adjacent solutions. Finally, the overall crowding distance value is calculated as the sum of individual distance values corresponding to each objective, and here each objective function is normalized before calculating the crowding distance.

Step 5. Creation of the offspring population by using binary tournament selection, recombination, and mutation operators. In this step, the simulated binary cross simulated binary crossover operator and polynomial mutation [30] are used.

Step 6. A combined population is formed by the parent and offspring populations, and this population is sorted into all different nondominated fronts.

Step 7. New population members are chosen. In the combined population, the solutions belonging to the first nondominated front are of best solutions, and all members of this front are definitely chosen in the new population. If the size of first nondominated front is smaller than the population size, the remaining members of new population are chosen from subsequent nondominated fronts in the order of their ranking. This procedure is continued until no more nondominated fronts can be accommodated. Generally, the count of solutions in the chosen nondominated fronts would be larger than the population size, we sort the solutions of the last chosen in descending order of crowding distance and choose the best solutions to fill the new population.

Step 8. Evolution is stopped when the generation is reached, otherwise this program goes back to Step 3.



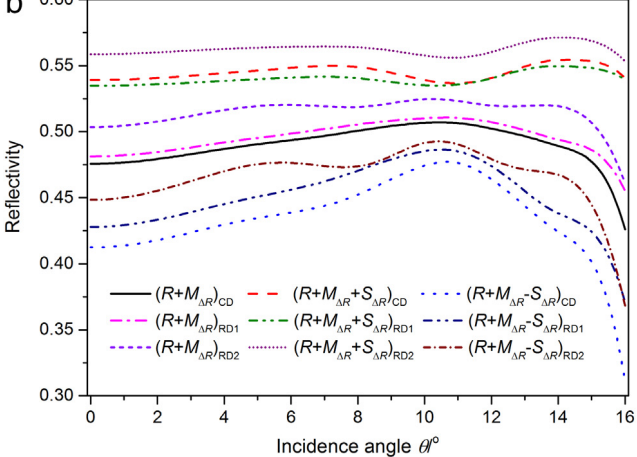


**Fig. 2.** (a) Theoretical reflectance of conventional and robust designs of Mo/Si multilayer with a broad incidence angular of reflection. The conventional design is obtained by only optimizing the reflectivity performance of designed multilayer, and these two robust designs are corresponding to boundary solutions in the nondominated front as shown in **Fig. 1**; (b) Mathematical expectation reflectance  $R+M_{AR}$  and the standard deviation corridor  $R+M_{AR}\pm S_{AR}$  of conventional design (CD) and robust designs, and the robust designs include robust design 1 (RD1) and robust design 2 (RD2), which are shown in **Fig. 1**. Here the random thickness error of Mo or Si layer has the normal distributions and standard deviations of 0.1 nm.

### 3. Results and discussions

In the following, the designs of two typical broadband Mo/Si multilayers have been considered, the first one has a constant reflectivity at wavelength of 13.5 nm in the incidence angular from 0° to 16° [10], and the second one has a constant reflectivity in a wavelength range from 13 nm to 15 nm [4,12]. It is worthwhile to point out that the calculation procedures of reflectivity above mentioned can be used in the simulations of these two kinds of broadband multilayers, and in our calculations, both designs of multilayers consist of 98 layers of Mo and Si which require thickness optimizations in the range between 1.5 nm and 4.5 nm. When the first kind of broadband multilayer is designed, the parameter  $\varphi$  in Eq. (8) corresponds to the incident angle  $\theta$ , while the second kind of broadband multilayer is simulated, the parameter  $\varphi$  corresponds to the incident beam wavelength  $\lambda$ . In the realistic multilayer system, the reflectivity is sensitive to the imperfections of interface [31], the interlayers [6,10,13,31] and the oxidation of top layer [10,32], thus in the simulations, we consider all these effects. For simplicity and without loss generality, we assume these two interlayers have the same chemical composition of MoSi2 and the fixed layer thicknesses, and the thicknesses of the Mo-on-Si and Si-on-Mo interfaces are 1.0 nm

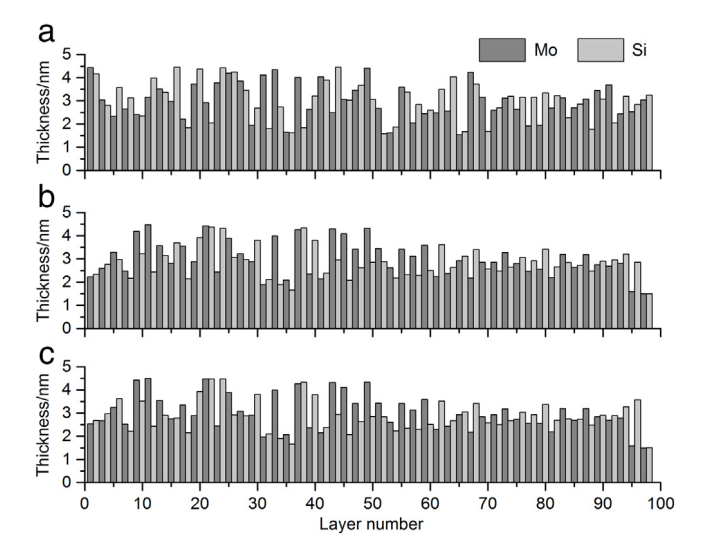


**Fig. 3.** Designed layer thickness distributions of Mo/Si multilayers with a broad incidence angular of reflection. (a) Conventional design; (b) and (c) are Robust designs 1 and 2 respectively, which are boundary solutions in the nondominated front as shown in Fig. 1. The naturally formed interlayers are considered, and the thicknesses of the Mo-on-Si and Si-on-Mo interfaces are 1.0 nm and 0.5 nm respectively, but these interlayers are not shown at this graph.

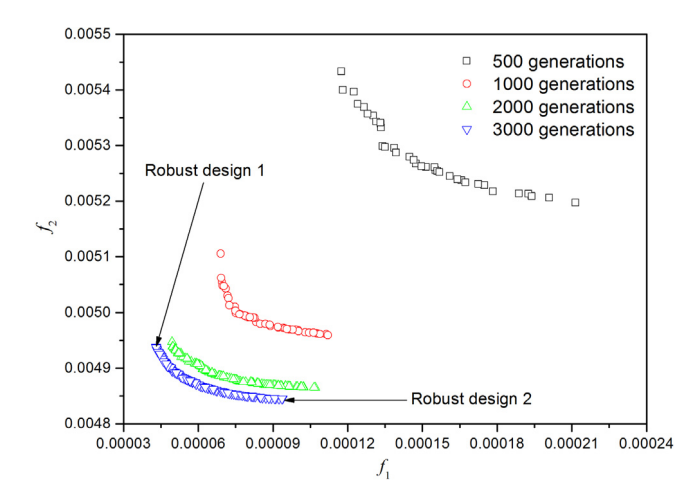


**Fig. 4.** Obtained nondominated solutions according to different generations of NSGA-II, where reflectivity and robust performances of multilayer designs are set as two optimized objectives. The designed target of reflectivity performance of Mo/Si multilayer is the constant reflectivity  $R_0 = 26\%$  in the range of wavelength [13 nm,15 nm] at a incidence angle of 1.5°. These two boundary solutions in the nondominated front are defined as "Robust design 1" and "Robust design 2", respectively. Here the random thickness error of Mo or Si layer has the normal distributions and standard deviations of 0.1 nm.

and 0.5 nm, respectively [6,31]. Therefore, the structure of multilayer system could be written as sub/[MoSi<sub>2</sub>/Mo/MoSi<sub>2</sub>/Si]<sub>49</sub>/SiO<sub>2</sub>, where SiO<sub>2</sub> oxide layer results from the oxidation of the top silicon layer with a thickness of 2 nm and a surface roughness of 0.6 nm. Furthermore, we assume the densities of all materials are the same as their bulk densities, and the interfacial roughness is 0.3 nm. As a result, this multilayer system we considered should be an appropriate model for the Mo/Si multilayer deposited by DC magnetron sputtering [6,13,31].

In the robust design of Mo/Si multilayer, we consider the random thickness errors of Mo and Si layers, which originate from the imprecise thickness controls, and it is assumed that the errors have the normal distributions and standard deviations of 0.1 nm. Using the multi-objective evolutionary algorithm, we firstly consider the robust design of Mo/Si multilayer with a broad incidence angular of reflection, and the nondominated solutions according to different generations are

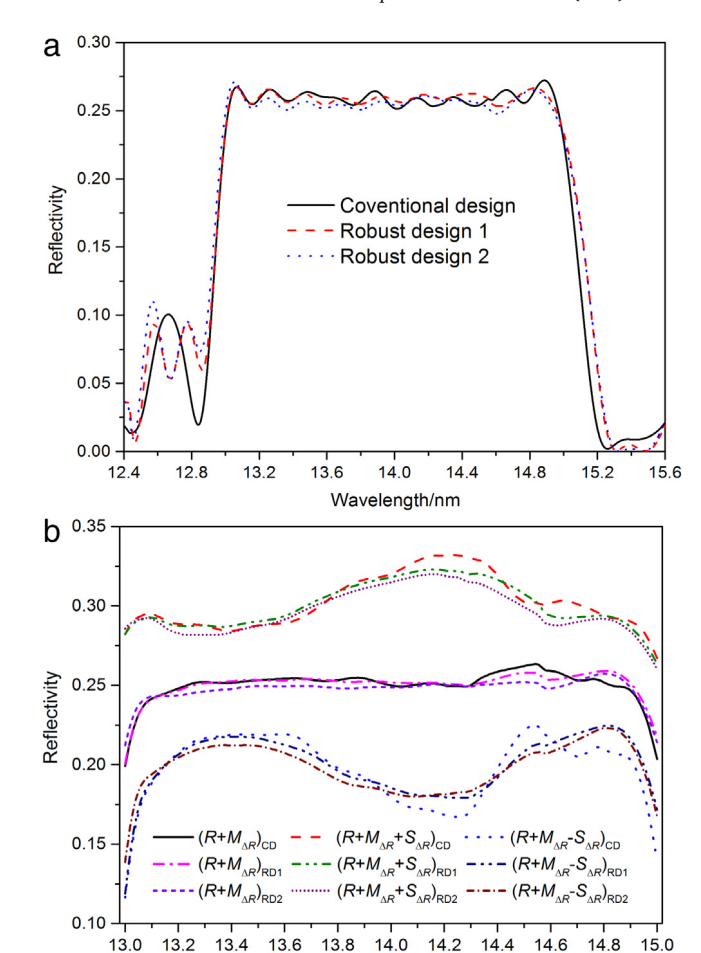


**Fig. 5.** (a) Theoretical reflectance of conventional and robust designs of Mo/Si multilayer with a broad wavelength of reflection. The conventional design is obtained by only optimizing the reflectivity performance of designed multilayer, and these two robust designs are corresponding to boundary solutions in the nondominated front as shown in **Fig. 4**; (b) Mathematical expectation reflectance  $R+M_{AR}$  and the standard deviation corridor  $R+M_{AR}\pm S_{AR}$  of conventional design (CD) and robust designs, and the robust designs include robust design 1 (RD1) and robust design 2 (RD2), which are presented in **Fig. 4**. Here the random thickness error of Mo or Si layer has the normal distributions and standard deviations of 0.1 nm.

Wavelength/nm

demonstrated in Fig. 1. An investigation of Fig. 1 shows that reflectivity and robust performances of design multilayer can be optimized simultaneously, and all individuals are in the first nondominated front after 500 generations. In the nondominated front, the solution having the best reflectivity performance has the worst robust design quality, while the solution having the best robust design quality supplies the worst reflectivity performance, and this phenomenon demonstrates the restrictive relation between these two performances of design multilayer. Therefore, we focus on two representative solutions which locate at the boundaries of nondominated front, and their corresponding theoretical reflectivity profiles are given in Fig. 2(a). For the sake of convenience and clarity, we define the boundary solution having the best reflectivity performance as "robust design 1", and the boundary solution having the best robust performance is defined as "robust design 2". For a comparison, the theoretical reflectivity of multilayer design which is obtained by only optimizing the reflectivity performance is shown in Fig. 2(a), and this multilayer design is defined as "conventional design". After an investigation of Fig. 2(a), it is found that the reflectivity profile of robust design 1 is nearly the same as that of conventional design, but the reflectivity profile of robust design 2 has much more fluctuations. Considering the influences of thickness errors of Mo and Si layers on

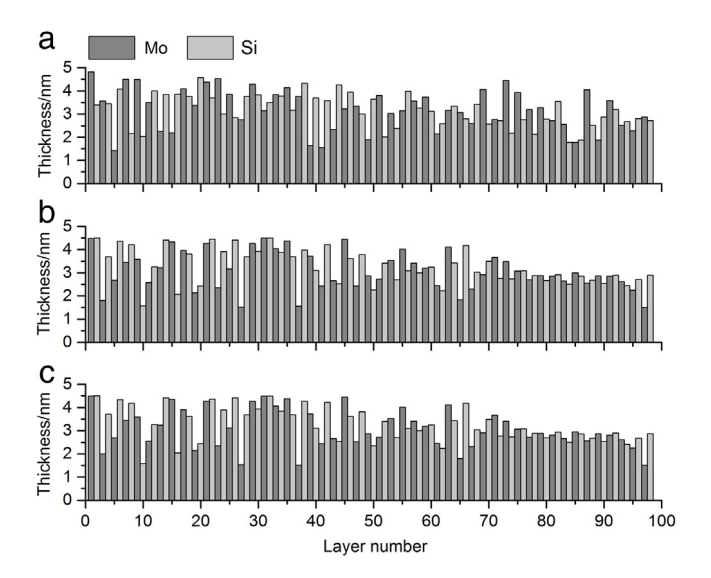


**Fig. 6.** Designed layer thickness distributions of Mo/Si multilayers with a broad wavelength of reflection. (a) Conventional design; (b) and (c) are Robust designs 1 and 2 respectively, which are boundary solutions in the nondominated front as shown in Fig. 4. The naturally formed interlayers are considered, and the thicknesses of the Mo-on-Si and Si-on-Mo interfaces are 1.0 nm and 0.5 nm respectively, but these interlayers are not shown at this graph.

reflectivity profile, the mathematical expectation reflectivity profile and corresponding standard deviation corridor of multilayer design can be given by [33]

$$M_{\Delta R}(\theta) = \frac{1}{2} \sum_{i=1}^{98} \frac{\partial^2 R(\theta)}{\partial d_i^2} \delta_i^2;$$

$$S_{\Delta R}^2(\theta) = \sum_{i=1}^{98} \left(\frac{\partial R(\theta)}{\partial d_i}\right)^2 \delta_i^2 + \frac{1}{4} \sum_{i,j=1}^{98} \left(\frac{\partial^2 R(\theta)}{\partial d_i \partial d_j}\right)^2 \delta_i^2 \delta_j^2, \tag{9}$$

where  $d_i$ ,  $d_j$ ,  $\delta_i$ ,  $\delta_j$  are thicknesses and thickness error's standard deviations of the *i*th and *j*th layers respectively, and  $M_{AB}$  and  $S_{AB}$  are deviation and variance of mathematical expectation reflectivity. The mathematical expectation reflectivity profiles and standard deviation corridors of these multilayer designs above mentioned are given in Fig. 2(b). An investigation of Fig. 2(b) presents that mathematical expectation reflections of robust designs are higher than that of conventional design, and the standard deviation corridor of robust design 1 is contained in that of conventional design. It means that the reflectivity performance of robust design has a lower sensitivity to the thickness errors than the conventional design, and then the robust design can be useful to reduce the production risks of EUV mirrors. Furthermore, the layer distributions of these multilayer designs are demonstrated in Fig. 3, and it is shown that the layer thickness distributions of robust design are completely different with that of conventional design, and there are several layers with different thicknesses between robust design 1 and robust design 2. The reason for this result is that solution search strategy of multi-objective algorithm is different with that of single objective algorithm. It is worthwhile to point out that every multilayer design which corresponds with solution between these two boundary solutions in the nondominated front has a lower sensitivity to random layer thickness variations than conventional design, and one can chose the appropriate design depending on the requirement of reflectivity performance and precision of deposited control.

Secondly, we consider the robust design of broadband Mo/Si multilayer with a wide spectral range of reflection, and nondominated solutions according to different generations are presented in Fig. 4. Fig. 4 depicts that reflectivity and robust performances of design multilayer can also be optimized simultaneously, and the nondominated solutions have a better convergence than the solutions in Fig. 1. Therefore, the

restrictive relation between reflectivity and robust performances of broadband spectral multilayer is not serious as that of multilayer with a broad incidence angular of reflection. However, we also concentrate on the boundary solutions in the nondominated front, and the boundary solutions with best reflectivity and robust performances are defined as "robust design 1" and "robust design 2", respectively. In Fig. 5(a), the theoretical reflectivities of these two robust designs are presented, and the theoretical reflectivity of "conventional design" of broad spectral multilayer which is obtained by only optimizing the reflectivity performance is also given to make a comparison. After an investigation of Fig. 5(a), it is found that the reflectivity plateaus of robust design and conventional design are similar, and the reflection bandwidths of robust designs are broader. When random thickness errors of Mo and Si layers are considered, the mathematical expectation reflectivity profile and standard deviation corridor of multilayer design can also be calculated by Eq. (9), but the incident angle  $\theta$  should be replaced by incident beam wavelength  $\lambda$ , and these results of robust and conventional designs are shown in Fig. 5(b). An investigation of Fig. 5(b) demonstrates that most part of standard deviation of corridor of robust design 2 is contained in that of conventional design, thus this robust multilayer design can be useful to increase the probability of production of high-quality Mo/Si mirrors. Moreover, these designed layer thickness distributions of robust and conventional designs are demonstrated in Fig. 6, and the layer thickness distributions are strikingly different between robust and conventional multilayer designs. Only a few of layers have different thicknesses between these two robust multilayer designs, and this result is consistent with the better convergence of solutions as shown in Fig. 4. Therefore, the design multilayer with a broad spectral reflection has a lower sensitivity to the random layer thickness variations than the design multilayer with a wide incidence angular of reflection.

### 4. Conclusion

A multi-objective evolutionary algorithm is applied in the robust design of broadband Mo/Si multilayer, and the reflectivity and robust performances of design multilayers are set as two optimized objectives. During the running of this algorithm, these two performances of design multilayer can be optimized simultaneously, and a set of robust designs of aperiodic multilayers can be obtained in one single simulation run. In our simulation, a more suitable model of Mo/Si multilayer is used, and the designing multilayer structures with a reduced sensitivity to random layer thickness variations can be conducive to reduce production risks of EUV mirrors. Moreover, this research has demonstrated a great potential of multi-objective evolutionary algorithm in the design of complex optical thin film.

### Acknowledgments

This project was supported by the National Natural Science Foundation of China (No. 61405189) and Jilin Scientific and Technological Development Plan (Nos. 20150101019JC and 20170312024ZG)

### References

- [1] C. Montcalm, R. Grabner, R. Hudyma, M. Schmidt, E. Spiller, C. Walton, M. Wedowski, J. Folta, Atomic-precision multilayer coating of the first set of optics for an extreme-ultraviolet lithography prototype system, Appl. Opt. 41 (2002) 3262–3269.
- [2] R. Soufli, R. Hudyma, E. Spiller, E. Gullikson, M. Schmidt, J. Robinson, S. Baker, C. Walton, J. Taylor, Sub-diffraction-limited multilayer coating for the 0.3 numerical aperture micro-exposure tool for extreme ultraviolet lithography, Appl. Opt. 46 (2007) 3736–3746.
- [3] H. Glatzel, D. Ashworth, M. Bremer, R. Chin, K. Cummings, L. Girard, M. Goldstein, E. Gullikson, R. Hudyma, J. Kennon, B. Kestner, L. Marchetti, P. Naulleau, R. Soufli, E. Spiller, Projection optics for extreme ultraviolet lithography (EUVL) micro-field exposure tools (METs) with a numerical aperture of 0.5, Proc. SPIE 8679 (2013) 867917-1-867917-16.
- [4] T. Feigl, S. Yulin, N. Benoit, N. Kaiser, EUV multilayer optics, Microelectron. Eng. 83 (2006) 703–706.

- [5] Y. Yao, H. Kunieda, H. Matsumoto, K. Tamura, Y. Miyata, Design and fabrication of a supermirror with smooth and broad response for hard X-ray telescopes, Appl. Opt. 52 (2013) 6824–6833.
- [6] E. Visnyakov, F. Kamenets, V. Kondratenko, M. Luginin, A. Panchenko, Y. Pershin, A. Pirozhkov, E. Ragozin, Aperiodic multilayer structures in soft X-ray radiation optics, Ouan. Elect. 42 (2012) 143–152.
- [7] A. Wonisch, U. Neuhaüsler, N. Kabachnik, T. Uphues, M. Uiberacker, V. Yakovlev, F. Krausz, M. Drescher, U. Kleineberg, U. Heinzmann, Design, fabrication, and analysis of chirped multilayer mirrors for reflection of extreme-ultraviolet attosecond pulses, Appl. Opt. 45 (2006) 4147–4156.
- [8] T. Kuhlmann, S. Yulin, T. Feigl, N. Kaiser, H. Bernitzki, H. Lauth, Design and fabrication of broadband EUV multilayer mirrors, Proc. SPIE 4688 (2002) 509–515.
- [9] A. Michette, Z. Wang, Optimization of depth-graded multilayer coatings for broadband reflectivity in the soft X-ray and EUV regions, Opt. Comm. 177 (2000) 47–55.
- [10] Y. Yakshin, I. Kozhevnikov, E. Zoethout, E. Louis, F. Bijkerk, Properties of broadband depth-graded multilayer mirrors for EUV optical systems, Opt. Express 18 (2010) 6957–6971.
- [11] P. Binda, F. Zocchi, Genetic algorithm optimization of X-ray multilayer coatings, Proc. SPIE 5536 (2004) 97–108.
- [12] S. Yulin, T. Kuhlmann, T. Feigl, N. Kaiser, Spectral reflectance tuning of EUV mirrors for metrology applications, Proc. SPIE 5037 (2003) 286–293.
- [13] A. Aquila, F. Salmassi, F. Dollar, Y. Liu, E. Gullikson, Development in realistic design for aperiodic Mo/Si multilayer mirrors, Opt. Express 14 (2006) 10073–10078.
- [14] M. Suman, F. Frassetto, P. Nicolosi, M. Pelizzo, Design of aperiodic multilayer structures for attsecond pulses in the extreme ultraviolet, Appl. Opt. 46 (2007) 8159–8169.
- [15] M. Pelizzo, M. Suman, G. Monaco, P. Nicolosi, D. Windt, High performance EUV multilayer structures insensitive to capping layer optical parameters, Opt. Express 16 (2013) 15228–15237.
- [16] Z. Wang, J. Zhu, B. Mu, Z. Zhang, F. Wang, X. Cheng, F. Wang, L. Chen, Development of non-periodic multilayer in the EUV, soft X-ray, and X-ray ranges, Chin. Opt. Lett. 8 (2010) 163–166.
- [17] M. Tan, H. Li, Q. Huang, H. Zhou, T. Huo, X. Wang, J. Zhu, Mo/Si aperiodic multilayer broadband reflective mirror for 12.5–28.5 nm wavelength range, Chin. Opt. Lett. 9 (2011) 023102-1–4.

- [18] I. Kozhevnikov, I. Bukreeva, E. Ziegler, Design of X-ray supermirrors, Nucl. Instrum. Methods Phys. Res. Sec. A 460 (2001) 424–443.
- [19] C. Morawe, E. Ziegler, J. Peffen, I. Kozhevnikov, Design and fabrication of depth-graded X-ray multilayers, Nucl. Instrum. & Methods Phys. Res. Sec. A 460 (2002) 189–198.
- [20] D. Burenkov, Y. Uspenskii, I. Artuyukov, A. Vinogradov, Algorithm for calculating the optimal parameters of multilayer aperiodic mirrors for soft X-ray, Quan. Elect. 35 (2005) 195–199.
- [21] Z. Wang, H. Wang, J. Zhu, F. Wang, Z. Gu, L. Chen, A. Michette, A. Powell, S. Pfauntsch, F. Schäfers, Broad angular multilayer analyzer for soft X-ray, Opt. Express 14 (2006) 2533–2538.
- [22] I.V. Kozhevnikov, A.E. Yakshin, F. Bijkerk, Wideband multilayer mirrors with minimal layer thicknesses variation, Opt. Express 23 (2015) 9276–9283.
- [23] H. Jiang, A. Michette, Robust design of broadband EUV multilayer beam splitters based on particle swarm optimization, Nucl. Instrum. & Methods Phys. Res. A 703 (2013) 22–25.
- [24] H. Greiner, Robust optical coating design with evolutionary strategies, Appl. Opt. 35 (1996) 5477–5483.
- [25] S. Wu, X. Long, K. Yang, Novel robust design method of multilayer optical coatings, ISRN Opt. 2012 (2012) 659642-1–6.
- [26] V. Pervak, M. Trubetskov, A. Tikhonravov, Robust synthesis of dispersive mirrors, Opt. Express 19 (2011) 2371–2380.
- [27] K. Deb, A fast and elitist multiobjective genetic algorithm: NSGA-II, IEEE Trans. Evol. Comput. 6 (2002) 182–197.
- [28] B. Henke, E. Gullikson, J. Davis, X-ray interactions: Photoabsorption, scattering, transmission, and reflection at E=50-30000eV, Z=1-92, At. Data Tables 54 (1993) 181–342.
- [29] A. Gibaud, S. Hazra, X-ray reflectivity and diffuse scattering, Curr. Sci. 78 (2000) 1467–1477.
- [30] K. Deb, R. Agrawal, Simulated binary crossover for continuous search space, Complex Syst. 9 (1995) 115–148.
- [31] S. Bajt, D. Stearn, P. Kearney, Investigation of the amorphous-to-crystalline transition in Mo/Si multilayers, J. Appl. Phys. 90 (2001) 1017–1025.
- [32] A. Aschentrup, W. Hachmann, T. Westerwalbesloh, Y. Lim, U. Kleineberg, U. Heinzmann, Determination of layer-thickness fluctuations in Mo/Si multilayers by cross-sectional HR-TEM and X-ray diffraction, Appl. Phys. A 77 (2003) 607–611.
- [33] S. Furman, A. Tikhonravov, Basics of Optics of Multilayer Systems, Edition Frontieres, 1992, pp. 58–68.